31st Annual International Conference of the IEEE EMBS
Minneapolis, Minnesota, USA, September 2-6, 2009

On spatio-temporal component selection in Space-Time Independent Component Analysis: An application to ictal EEG

Christopher J. James*, *Senior Member, IEEE* and Charmaine Demanuele, *Student Member, IEEE*

***Abstract*—This paper assesses the use of Independent Component Analysis (ICA) as applied to epileptic scalp electroencephalographic (EEG) recordings. In particular we address the newly introduced Spatio-Temporal ICA algorithm (ST-ICA), which uses both spatial and temporal information derived from multi-channel biomedical signal recordings to inform (or update) the standard ICA algorithm. ICA is a technique well suited to extracting underlying sources from multi-channel EEG recordings – for ictal EEG recordings, the goal is to both de-noise the EEG recordings (i.e. remove artifacts) as well as isolate and extract epileptic processes. As part of any ICA application, there is an interim stage whereby relevant components (or processes) need to be identified – either objectively or subjectively (usually the latter). In previous work with ST-ICA we used spectral information alone to identify the underlying processes subspaces extracted by the ST-ICA. Here we assess the joint use of spatial as well as spectral information for this purpose. We test this on ictal EEG segments where it can be seen that different underlying processes possess characteristic signatures in both modalities which can be utilized for the clustering (or process selection) stage.**

I. Introduction

Electroencephalography is a valuable tool for the diagnosis and prognosis of epilepsy, a potentially debilitating disorder characterized by sudden and recurrent brain dysfunction known as epileptic seizures. Multi-channel electroencephalographic (EEG) recordings are often acquired in dedicated Epilepsy Monitoring Units to be visually inspected by clinical experts whom, through training and experience, extract features of relevance from the recordings. One of the aims of this exercise is to identify the region(s) of the brain where the seizure is at its onset and to determine which brain regions are activated during the course of the seizure. This is essential for cases which are candidates for surgery. However, such manual inspection is often a long and cumbersome process since seizure components are superimposed on noisy 'ongoing' background EEG. The seizure level is below this ongoing level at seizure onset and is then contaminated by strong ocular, muscular and cardiac activity as well as disturbances from electrode movements as the seizure evolves.

Over the years ensemble (spatial) independent component analysis (E-ICA) [1] has been successfully employed to de-noise and extract seizure components, manifest predominantly as rhythmic activity, from the raw scalp multichannel EEG [2]. E-ICA is a statistical technique which performs Blind Source Separation (BSS) on linear mixtures of statistically independent sources in order to isolate spatially distinct independent components (ICs) from the data. However, this technique is limited by the fact that each extracted IC has a spatial topography that is fixed in time, whereas the seizure focus may change over time and its activity may spread to other brain areas. Consequently, spatio-temporal techniques are of great clinical relevance for the analysis of ictal EEG, where the multi-dimensional nature of the recordings in addition to the rich dynamical time structure of EEG data can be used to track changes in the spatial distribution and morphology of the epileptic sources over time. In [3-4] we introduced a new algorithm – Space-Time ICA (ST-ICA) – which uses spatial as well as temporal/spectral information to solve the BSS problem. This is an augmentation of Single-Channel ICA (SC-ICA), which is a purely temporal ICA source model that is able to extract multiple underlying sources from a scalar time series where only single channel recordings are available or desirable [5].

In this paper we briefly revisit the framework whereby source analysis is undertaken through the use of spatio-temporal information to inform the standard ICA algorithm. We particularly assess the effectiveness of both spatial and spectral information that is extracted from the recorded data as part of the ST-ICA procedure. Specifically we investigate ways of utilizing both spatial and spectral contextual cues as a means of identifying the subspaces pertaining to the underlying sources or processes.

II. Materials And Methods

A. Ensemble (Spatial) ICA: E-ICA

E-ICA (a.k.a. spatial ICA) represents the 'standard' ICA source model. In this model, the sensor measurements $x(t) = [x_1(t), ..., x_p(t)]^T$ are assumed to be made up of a linear instantaneous mixture of independent sources, $s(t) = [s_1(t), ..., s_q(t)]^T$, such that $x(t)=As(t)$ where A denotes the [pxq] mixing matrix, and (p≥q). ICA aims to find an unmixing matrix W, ($W = A^{-1}$), in order to demix the measurements such that $y(t)=Wx(t)$, where the q-dimensional vector $y(t)$ contains the ICs which are estimates of the underlying sources. The estimation of W is simplified by means of the whitening (decorrelation) procedure, which makes the covariance matrix of $x(t)$ diagonal and its

*C.J. James is with the Signal Processing and Control Group, ISVR, University of Southampton, SO17 1BJ, UK, (Tel: +44 (0)2380 593043; Fax: +44 (0) 23 8059 3190; e-mail: C.James@soton.ac.uk). C. Demanuele is with the Signal Processing and Control Group, ISVR, University of Southampton, SO17 1BJ, UK (cd3@soton.ac.uk).

components of unit variance. FastICA is one of many implementations of ICA found in the literature [6], which is often employed for its ease of implementation and speed of operation [7].

B. Single-Channel ICA: (SC-ICA)

For the implementation of SC-ICA, a multidimensional representation of the measured signal $x(t)$ is achieved by constructing a delay matrix $Q(t)$ from a set of m-dimensional delay vectors X_t, such that

$$X_t = \left[x(t), x(t+\tau), ..., x(t+(m-1)\tau)\right]^T,$$
$$Q(t) = \left[X_t, X_{t+\tau}, ..., X_{t+N\tau}\right] \quad (1)$$

where τ is a lag term, m is the number of lags a.k.a. the embedding dimension, and N is the length of the time series [5]. We set τ to 1 and m to 95 based on previous work on this data-set [3]. FastICA is applied to the delay matrix to learn A, W and a set of ICs in the source space, s, these being estimates of the underlying sources. The delay matrix of the estimated sources is then projected back onto the measurement space by means of a mixing-unmixing process, to form $\tilde{Q}$

$$Q = As, \quad s = WQ, \quad \tilde{Q} = AWQ. \quad (2)$$

Since this is a purely temporal ICA source model, the columns of A and the corresponding rows of W contain the impulse response of m FIR filters, covering a number of generating filters and their shifted versions. Filters with the same magnitude frequency response $|f_i(\omega)|$ (but different phase responses) are grouped into C subsets γ_p spanning linearly independent subspaces E_p,

$$f_p(t) = \sum_{i \in \gamma_p} |f_i(\omega)|, \text{ (where } f_i = A_{(:,i)} W_{(i,:)}). \quad (3)$$

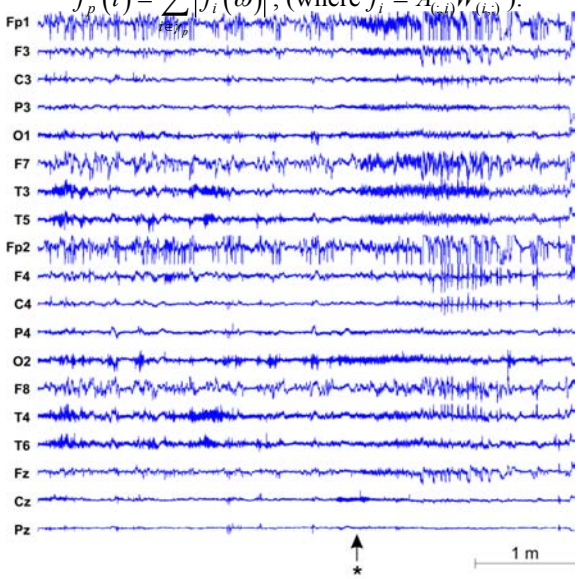

Fig. 1: A 5 minute segment of multi-channel ictal EEG is depicted, a seizure with a sudden left fronto-temporal onset occurs at the point indicated by the marker (*). The recording is severely contaminated with ocular artifact throughout.

Q is passed through these filters, $\tilde{Q}_p(t) = f_p.Q$, to form the independent processes $\{P_1 ... P_C\}$ spanned by $\{E_1, ... E_C\}$. Therefore, each process P_i spanned by subspace E_i is manifested in the measurement space by a matrix of delays $\tilde{Q}_i$. Moreover, since this is a lossless procedure, summing $\{\tilde{Q}_1, ..., \tilde{Q}_C\}$ returns the original time delay matrix Q. These delay matrices are then unembedded to form the one-dimensional, independent process time-series. Note that the mapping of a scalar time series into a multidimensional model implies that the processes can only be successfully indentified provided that they have disjoint spectral support.

C. Space-Time ICA: (ST-ICA)

This is an extension of the SC-ICA method, whereby the matrix of delays is constructed from n channels of interest such that the new overall delay matrix Q^{tot} becomes

$$Q^{tot} = \left[\left(Q^1\right)^T ... \left(Q^n\right)^T\right]^T. \quad (4)$$

Thus, for an n-channel system of N samples per channel, Q^{tot} has dimension (nm x (N-m+1)). Again, this matrix is decomposed into its constituent underlying independent processes through FastICA. In this case, the ICA algorithm learns matrices A and W, each column and row containing n superimposed filters, which have similar *but not identical* frequency responses due to possible subtle variations of the underlying sources in different spatial locations. In this way, there is an FIR filter for every selected scalp location, representing full spatial-temporal filtering. Some of the columns of A and corresponding rows of W represent repeated FIR filters pertaining to the same independent process (and hence spanning the same subspace), which can be grouped together to form C sets of n generating filters – i.e. a mixing filter per measurement channel. The multichannel projections of the underlying independent processes $\{P_1 ... P_C\}$ are then obtained by filtering and unembedding, as for the single-channel case.

D. Clustering the spatio-temporal filters

ST-ICA uses temporal information inherent in scalar time series (as in SC-ICA) but it also incorporates the spatial information inherent within the augmented delay matrix Q^{tot} in the separation process. Therefore, we have a wealth of information about the spectral characteristics, the temporal dynamics and the spatial distribution of the extracted processes. This also implies that after the ICA process we are able to cluster the filter banks based on *either* similar frequency responses *or* on comparable spatial patterns (or indeed using both). To date, we cluster based only on the similarity of the magnitude frequency responses (the Power

Spectral Density – PSD), but both scenarios need to be investigated to ensure that we exploit all the information provided by this technique. This paper assesses, for the first time, the information content of both the PSDs of the filter banks as well as the spatial distribution of this information in order to select C subspaces that contain the underlying processes, P_C.

E. Epileptiform Data

We analysed multi-channel ictal scalp EEG recordings of a number of patients who were undergoing continuous scalp EEG monitoring for possible epileptic surgery. We studied 5-minute seizure segments, including a pre-ictal period of 3 minutes. The data was recorded using nineteen electrodes placed on the scalp according to the International 10-20 electrode placement system, using reference FCz. The data was sampled at 200 Hz at 12 bit resolution and digitally stored. Figure 1 depicts one such example of an ictal EEG segment with a rhythmic seizure component of a left fronto-temporal origin occurring about 3 minutes into the segment. Note that the segment is severely contaminated with ocular artifact throughout.

III. RESULTS

The ST-ICA process described in the previous section was applied to the data after first subtracting the mean value of each recording, and then reducing the dimensionality of the data matrices through SVD to a dimension of 40 (obtained after observing the structure of the singular-spectrum and choosing a value which depicts the start of the noise floor).

After the spatio-temporal matrix of delays Q^{tot} is obtained and FastICA applied, the columns of the mixing matrix A are scrutinized with respect to the spatial and spectral information they contain. Figure 2 depicts the PSDs of the impulse response of each FIR filter (one per channel) for a set of chosen ICs. Note that FastICA learns these multiple FIR filters, where each column of (n =19) filters corresponds to one IC. Multiple FIR filter columns must now be grouped in order to identify the underlying processes. Figure 2(a) depicts Group 1, made up of components 11, 18 and 21 which all exhibit similar spectral properties (a prominent peak in the PSDs at 6~7 Hz). The topography shown in the inset depicts the spatial distribution of the total power in each channel PSD for each component. For Group 1 there is a predominantly tight left fronto-temporal focus. The sub-topographies within each component show the distribution of power within the PSDs for 5 frequency bands from 0-2, 2-4, 4-6, 6-8, 8-10 Hz. These show that the different frequencies visible in the PSDs exhibit disparate spatial foci. Figure 2(b) depicts Group 2 made up of components 25 and 33 with similar PSDs yet different to those in Group 1. The spatial distribution of Group 2 is also more frontal than Group 1.

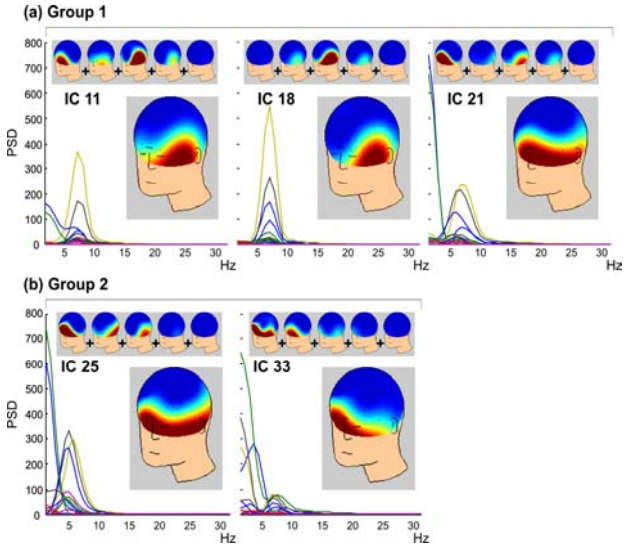

Fig. 2: Following the application of STICA the columns of the mixing matrix represent FIR filters, the PSDs of the responses of these filters are represented here for each channel for selected components. (a) Group 1: the PSDs of all channels for components 11, 18 & 21 exhibit similar properties. The topography inset shows the spatial distribution of the total power in each channel PSD for each component. The sub-topographies show the distribution of power for 5 frequency bands from 0-2, 2-4, 4-6, 6-8, 8-10 Hz. (b) Group 2: components 25 & 33 show PSDs with similar distributions (spectrally and spatially).

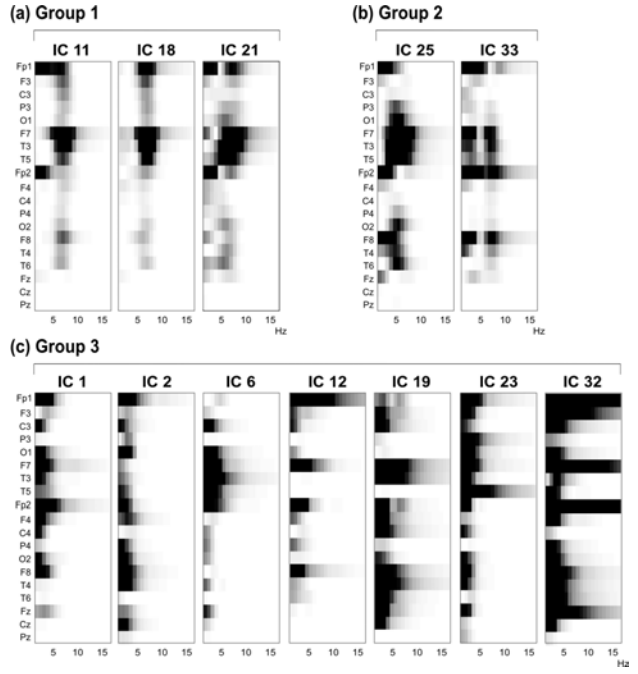

Fig. 3: Plots of PSD for selected components wrt spatial location of each respective FIR filter are show here. (a) Group 1 – ictal process 1: components 11, 18 & 21 exhibit similar spectral/ spatial distributions. (b) Group 2 – ictal process 2: components 25 & 33 depict similar spectral/ spatial distributions. (c) Group 3 – ocular process: 1, 2, 6, 12, 19, 23 & 32 exhibit varied distributions spatially but strongest at lower frequencies.

Figure 3 depicts plots of the PSDs for the same selected components as in Figure 2 (3(a) and 3(b)) and contrasts them with the components for an artifactual (ocular) process – Figure 3(c). The figures show the spectral response versus spatial location of each respective FIR filter, where a darker colour represents a stronger response. Note the similar overall spectral and spatial distributions for the ICs in each group. The artifactual group contains more ICs and the power is spread wider spatially yet concentrated in the lower frequency bands (typical of ocular artifacts).

Figure 4 depicts butterfly plots of three of the identified processes underlying the measured data. These were formed by defining the process subspaces using the components as noted in Figure 3, and then projecting back each group of components to the measurement space and unembedding the resultant matrices. In each case Group 1, 2 and 3 represent just three processes underlying the (mixed) measured EEG signals. Groups 1 and 2, depict ictal processes – note the onset times which are co-incident with the onset times in the raw recordings, and Group 3 shows ocular artifact, the amplitude and intensity of this artifact increases about 30 s into the seizure onset, this is evident in the raw recordings too.

IV. Discussion and Conclusions

In this paper we revisit previous work [3-4] where we introduced the concept of ST-ICA applied to ictal EEG data and compared it with ensemble ICA and SC-ICA methods. In previous work we showed that in ST-ICA both spatial and temporal information is used to inform the standard ICA algorithm and that this results in the ability to separate sources that are both spatially and spectrally overlapping, something which is only possible through ST-ICA. In previous work, the independent underlying processes were selected based upon the similarity of the PSD of the FIR filters that ICA learns in the ST-ICA model. This means that although spatial and temporal information is used in the ICA procedure, the clustering phase could be neglecting useful information and result in processes which are ill-defined. Here, we analyze both the spatial as well as the spectral content of the FIR filters – the PSDs and their spatial extent are observed and the underlying processes are defined based on the similarity of both quantities. Although preliminary at this stage, the results show that, for the most part, the PSDs of each FIR filter for a given IC are similar (although not identical). Moreover, for a given IC, some PSDs at specific spatial locations differ and indicate the potential of some remnant mixing remaining even after the ST-ICA decomposition (c.f. low-frequency components at frontal channel locations indicative of ocular artifacts.) This is possibly due to the close spatial proximity of the ictal source to the ocular artifactual source resulting in some remnant mixing. Future work will consider an automated clustering method that uses the spatial/spectral matrices shown in Figure 3 to identify the underlying processes.

References

[1] P. Comon, “Independent component analysis, A new concept?”, Signal Processing, vol. 36, pp. 287-314.

[2] C. J. James and C. W. Hesse, “Independent component analysis for biomedical signals”, Physiological Measurement, vol. 26, R15-R39, 2005.

[3] C.J. James, D. Abasolo, D. Gupta, “Space-time ICA versus Ensemble ICA for ictal EEG analysis with component differentiation via Lempel-Ziv complexity”, Proc. 29th Annu. IEEE EMBS Int. Conf., Lyon, France, 2007.

[4] C.J. James, “On independent component analysis based on spatial, temporal and spatio-temporal information in biomedical signals”, 4th European Congress for Medical and Biomedical Engineering, EMBEC 2008, Antwerp, Belgium; ECIFMBE Proceedings, vol. 22, pp.34-37, 2008.

[5] M.E. Davies and C.J. James, “Source separation using single channel ICA”, Signal Processing, vol. 87, pp. 1819-1832, 2007.

[6] A. Hyvärinen, J. Karhunen and E. Oja, "Independent Component Analysis", John Wiley and Sons, New York, 2001.

[7] A. Hyvärinen, and E. Oja, “A fast fixed-point algorithm for independent component analysis”, Neural Computation, vol. 9, pp. 1483-1492, 1997.

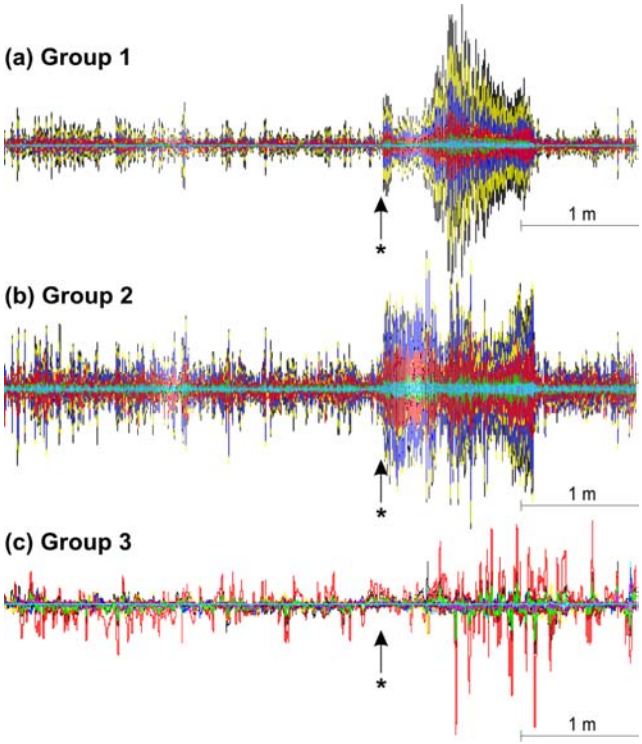

Fig. 4: Butterfly plots of three of the identified processes (projected to the measurement space) underlying the measured data. (a) Group 1 and (b) Group 2, depict ictal processes – note the onset times which are co-incident with the onset times in the raw recordings. (c) Group 3: ocular artifact, the amplitude and intensity of this artifact increases about 30 s into the seizure onset, this is evident in the raw recordings too.